Transcriptome Analysis Reveals the Potential Antioxidant Defense Mechanisms of Myzus persicae in Response to UV-B Stress

Changli Yang
Guizhou University
Changyu Zhang (zcy1121@aliyun.com)
Guizhou University https://orcid.org/0000-0002-1269-4615
Jianyu Meng
Guizhou Tobacco Science Research Institute
Mengshuang Yao
Guizhou University

Research article

Keywords: Myzus persicae, UV-B stress, RNA-seq, antioxidant mechanisms, metabolism, immune response

Posted Date: December 12th, 2019

DOI: https://doi.org/10.21203/rs.2.18311/v1

Abstract

Background: As an environmental stress factor, ultraviolet-B (UV-B) radiation directly affects the growth and development of Myzus persicae. Excessive UV-B stress leads to DNA, membrane lipid, and protein damage by the production of reactive oxygen species. However, M. persicae can adaptively respond to such environmental stress by activating the relevant mechanisms in the body. How M. persicae responds to UV-B stress and the molecular mechanisms underlying this adaptation remain unknown.

Results: Here, we compared and analyzed transcriptome data for M. persicae following exposure to a light-emitting diode fluorescent lamp and UV-B radiation for 30 min. We identified 758 significant differentially expressed genes (DEGs) following exposure to UV-B stress, including 423 upregulated and 335 downregulated genes. In addition, enrichment analysis using the Gene Ontology and Kyoto Encyclopedia of Genes and Genomes databases illustrated that these DEGs are associated with antioxidation and detoxification, metabolic and protein turnover, immune response, and stress signal transduction. Simultaneously, these DEGs are closely related to the adaptability to UV-B stress.

Conclusions: Our results suggest that UV-B stress is associated with a wide range of physiological effects in M. persicae. Our research can raise awareness of the mechanisms of insect responses to UV-B stress.

Background

In recent years, the destruction of the stratospheric ozone layer in the Earth's atmosphere has sharply increased interest in the effects of solar ultraviolet radiation on the Earth's surface, especially ultraviolet-B (UV-B) radiation with a wavelength of 280–320 nm [1]. UV-B is considered a widespread environmental stress factor that induces oxidative stress in organisms through the production of reactive oxygen species, causing DNA, membrane lipid, and protein damage [2–4]. Numerous studies illustrated that UV-B radiation has a wide range of effects on the growth, physiology, biochemistry, and population structure of organisms, and organisms can adopt both protection and repair strategies to adapt to UV-B stress [5, 6]. As an environmental stress factor, UV-B can cause oxidative stress and genetic mutations, leading to death of insects [7–10]. However, the molecular mechanisms by which insects adapt to UV-B stress are unclear.

The green peach aphid Myzus persicae (Sulzer) (Homoptera: Aphididae) is a worldwide pest that seriously harms > 400 plants such as tobacco, cruciferous vegetables, peppers, potatoes, eggplants, and melons. This pest can cause the leaves of plants to curl, wither, and even die, thereby reducing crop yields [11, 12]. It can also spread > 100 plant viruses as a viral vector and cause sooty blotch and mold parasitic infection through the secretion of honeydew, causing great losses in the production of cash crops [11]. M. persicae lives year-round under direct sunlight, but it is unable to escape from UV-B as an environmental stress factor.

Transcriptome sequencing is widely used in genomic analysis and functional gene identification to help understand the host's genetic response to UV-B stress and the molecular mechanisms of antioxidant

defense systems. In this study, functional transcripts of M. persicae under UV-B stress were identified via transcriptome sequencing analysis using the Illumina sequencing platform. The results further clarified the antioxidant mechanisms of M. persicae and explored the molecular mechanisms of insect adaptation to UV-B environmental stress, providing novel targets for the prevention and management of pests.

Results

mRNA sequencing, sequence assembly, and functional annotation

In total, 177,070,180 (26.56 Gb) raw reads were generated from the two libraries (control and UV-B radiation groups) using Illumina HiSeq™ 4000 sequencing technology, and 80,281,002 and 90,660,496 clean reads were obtained from the two groups, respectively, after quality control decontamination (Table 1). The data quality of the clean reads for the control and UV-B radiation groups were separately evaluated. The results illustrated that the Q30 quality score exceeded 92% for both groups. The GC contents of the two groups were 41.6% and 41.5%, respectively, and >93% of the clean reads were independently aligned on the *M. persicae* reference genome, and <4% of the clean reads of both groups had multiple alignment positions on the reference genome. In addition, the intron region, 5' UTR, 3' UTR, and CDS comprised 1.62%, 6.10%, 4.7%, and 83.72% of the clean reads in the control group, respectively, versus 2.01%, 7.03%, 4.4%, and 83.48%, respectively, in the UV-B radiation group. These clean reads were assembled to obtain 40,699 unigenes, and the length distribution of all unigenes is shown in Fig. 1. These results demonstrated that the sequencing quality was relatively high, indicating that the unigenes were suitable for subsequent annotation analysis. We then annotated our unigenes using six functional databases and found that 37,226 (91.47%), 25,478 (62.60%), 29,164 (71.66%), 5,366 (13.18%), 16,885 (41.49%), and 18,898 (46.43%) unigenes could be mapped to the NR, Swiss-prot, Pfam, COG, Gene Ontology (GO), and Kyoto Encyclopedia of Genes and Genomes (KEGG) databases, respectively.

Transcript expression analysis

To better classify the genes with different expression levels, genes were divided into three groups based on the FPKM value: high (FPKM > 10), medium (1 < FPKM ≤ 10), and low (0 < FPKM ≤ 1) (Table 2). The genes with high expression levels under UV-B stress may play important roles in the normal metabolism of *M. persicae*. The two libraries (control and UV-B radiation groups) included 7058 and 6611 genes with high expression, respectively (Table 2). UV-B stress had great influence on gene expression in *M. persicae*. Differential expression analysis identified 758 DEGs in the UV-B radiation group (423 upregulated, 335 downregulated) compared with their levels in the control group (Fig. 2).

GO and KEGG analyses of DEGs

We focused on 423 upregulated and 335 downregulated genes to further understand the biological mechanism by which *M. persicae* responds to UV-B stress. In GO analysis, we grouped DEGs into three categories, namely, biological process, cellular component, and molecular function (Fig. 3). In the biochemical process category, “metabolic process,” “cell process,” and “single biological process” were

significantly enriched. In the cell component category, “membrane,” “cell part,” “membrane part,” and “cell” were significantly enriched. In the molecular function category, “catalytic activity” and “binding” were significantly enriched. In addition we also found that 31 DEGs were significantly associated with the “response to stimulus.”

KEGG is a bioinformatics database for the systematic analysis of gene function [13]. In this study, 576 DEGs were annotated into 194 pathways, which were further divided into six categories as follows: cellular processes, environmental information processing, genetic information processing, metabolism, organismal systems, and human metabolism diseases. The first 62 KEGG pathways are shown in Fig. 4. Among these pathways, the immune and antioxidant defense, transport and catabolic, and signal transduction pathways were mainly enriched.

Antioxidant and detoxification

In this study, we identified several genes involved in the regulation of antioxidant and detoxification mechanisms (Fig. 5). Seven DEGs in the peroxisome pathway were associated with antioxidant systems [14]. In this pathway, fatty acyl-CoA reductase (Unigene 15357 and Unigene 11089), hydroxymethylglutaryl-CoA lyase (Unigene 5738), mpv17-like protein 2 (Unigene 7104), and long-chain-fatty-acid-CoA ligase five genes (Unigene 9666) were upregulated, and two fatty acyl-CoA reductase genes (Unigene 7287 and Unigene 7290) were downregulated. In addition, we identified DEGs associated with metabolic detoxification, including genes encoding glutathione S-transferase (up: MSTRG.2702; down: Unigene 11295, Unigene 1210, and MSTRG.2676), carboxylesterase (upregulated: Unigene 9292, Unigene 16134, Unigene 7342, Unigene 9915, Unigene 10148, and Unigene 6271; downregulated: Unigene 6278), aldehyde dehydrogenase (Unigene 1926), and cytochrome P450 (CYP).

Metabolic and protein turnover

In this study, many metabolic reactions were significantly enhanced under UV-B stress in *M. persicae*, including carbohydrate (12 pathways), lipid metabolism (13 pathways), cofactor and vitamin metabolism (6 pathways), and amino acid metabolism (12 pathways). Among them, genes induced in carbohydrate metabolism included those involved in pyruvate metabolism (three DEGs), tricarboxylic acid cycle (TCA cycle) (three DEGs), glycolysis/gluconeogenesis (two DEGs), ascorbic acid and metabolism (four DEGs), and starch and sucrose metabolism (five DEGs). Moreover, we found that some genes related to amino acid metabolism were induced, including those involved in alanine, aspartate, and glutamate metabolism (three DEGs); glycine, serine, and threonine metabolism (two DEGs); cysteine and methionine (two DEGs); valine, leucine, and isoleucine degradation (seven DEGs); lysine degradation (three DEGs); and arginine and proline metabolism (one DEG).

Immune response

In our study, many immune-related DEGs were significantly enriched, most of which were upregulated in response to UV-B stress. These genes were mainly involved in five pathways, including antigen

processing and presentation (17 DEGs), platelet activation (six DEGs), and chemokine signaling pathways (three DEGs) (Fig. 6). Nine, five, and two unigenes related to antigen processing and presentation, platelet activation, and chemokine signaling pathways, respectively, were upregulated. Among these, cathepsin B (CTSB) has 14 DEGs (6 unregulated and 8 downregulated) involved in the antigen processing and presentation pathways. In addition, some antiviral genes such as serine proteinase inhibitor 2 (Unigene 7537) and scavenger receptor class B (Unigene 10115) genes were induced. Fc gamma R-mediated phagocytosis (Unigene 7353) gene, which is involved in insect immunity, was upregulated.

Stress signal transduction

Many pathways involved in stress signal transduction were identified in our analysis, including PI3K-Akt (three DEGs), AMPK (three DEGs), Ras (two DEGs), Rap1 (three DEGs), calcium (two DEGs), cGMP-PKG (four DEGs), cAMP (five DEGs), and HIF-1 signaling pathways (two DEGs), the number of genes upregulated by these signaling pathways is one (Unigene12911); two (Unigene12911 and Unigene10827); one (Unigene177); one (Unigene979); one (Unigene3013); three (Unigene3013, Unigene9434 and Unigene12368); three (Unigene4952, Unigene4257, and Unigene12368); and one (Unigene6075), respectively.

Validation of expression profiles via qRT-PCR

To verify the transcriptome data, we randomly selected 15 genes and further tested their relative expression levels via qRT-PCR. According to comparative analysis, the trend of qRT-PCR results was consistent with the results of DEG expression analysis (Fig. 7), which verified the accuracy and reliability of the sequencing data.

Discussion

Most insects grow and multiply under direct sunlight and thus cannot escape the UV-B effect of direct sunlight. However, many insects also develop a variety of mechanisms, including morphological and physiological adaptations, in response to UV-B stress. This may be due to the expression of certain unique genes in the body of insects. In this study, we performed a comparative transcriptional analysis of M. persicae to identify genes associated with the UV-B adaptability of this species. We identified 758 DEGs under UV-B stress (423 upregulated and 335 downregulated) and analyzed numerous biomarkers for antioxidants and detoxification, metabolic and protein turnover, immune response, and stress signal transduction. In GO analysis, 31 DEGs were significantly associated with the “response to stimulus,” which is related to the response of M. persicae to UV-B stress. Similar results have been reported for response of Glyphodes pyloalis to heat stress and the response of Antheraea pernyi to zinc stress [15, 16]. In addition, 92 DEGs were associated with “membrane,” suggesting that most cells of M. persicae need to be repaired under UV-B stress [17].

UV can result in ROS accumulation in insect cells, and the imbalance between ROS production and antioxidation can directly lead to a variety of toxic effects, including non-specific DNA, protein, and lipid damage [3, 4, 18, 19]. Several antioxidant-related genes, fatty acyl-CoA reductase (Unigene 15357 and Unigene 11089), hydroxymethylglutaryl-CoA lyase (Unigene 5738), mpv17-like protein 2 (Unigene 7104), and long-chain-fatty-acid-CoA ligase were significantly upregulated after UV-B treatment (Fig. 5). These upregulated genes function as antioxidants to remove ROS in M. persicae. In addition, UV-B stress promotes the accumulation of toxic substances in M. persicae. Regarding detoxification and antioxidative mechanisms, glutathione S-transferase can catalyze the binding of the electrophilic group of endogenous harmful substances produced by UV-B stress to the thiol group of reduced glutathione, thereby forming a more soluble, non-toxic derivative that is easily excreted or decomposed by metabolic enzymes [20]. The activity of glutathione S-transferase in Helicoverpa armigera adults was also significantly increased under UV stress [18]. As an important serine hydrolase in insects, carboxylesterase can effectively catalyze the hydrolysis of various endogenous and exogenous compounds containing carboxyl ester bonds, amide bonds, and thioester bonds [21]. In our study, multiple carboxylesterase genes were significantly induced. The P450 enzyme system can metabolize various harmful endogenous and exogenous substances to protect living cells [22]. However, under UV-B stress in M. persicae, seven unique CYP sequences were induced, and these sequences were grouped into the CYP6 (four sequences), CYP4 (two sequences), and CYP18 clades (one sequence). CYP6BQ4 and CYP6BQ8 mRNA levels were also significantly increased under UV-A stress in Tribolium castaneum [23]. Therefore, the antioxidant and detoxification processes were speculated to be closely related to the response of M. persicae to UV-B stress.

Metabolism in insects plays a key role in environmental stress tolerance as the balance of energy demand and supply is crucial for survival. Our results indicated that the metabolism of M. persicae was enhanced under UV-B stress. Some genes related to TCA cycle, glycolysis, and pyruvate metabolism of M. persicae were significantly upregulated under UV-B stress. However, the TCA cycle and glycolysis are two important pathways for ATP production in insects; they are crucial for ensuring the energy supply of M. persicae in response to UV-B stress. Our results were consistent with those previously reported for Macrosiphum euphorbiae under UV-B stress and Drosophila melanogaster under UV-A stress [24, 25]. UV-B stress leads to the accumulation of pyruvate, which can effectively remove ROS, reduce protein carbonylation, and stabilize mitochondrial membrane potential; these findings are similar to those reported in fungi under UV stress [26, 27]. These specifically induced metabolism-related genes were involved in the adaptive mechanisms of M. persicae in response to UV-B stress.

Because insects lack adaptive immunity, they can only rely on innate immune reactions for defense; however, these reactions also cause immunological changes during the stress response [28, 29]. CTSB is an important proteolytic enzyme in insect lysosomes, which plays an important role in growth and metabolism by degrading protein activity and maintaining normal programmed cell death. As an important digestive protease present in various oviparous animals, CTSB provides nutrients for embryonic development by breaking down vitellin containing abundant amino acid components in the egg [30–34]. Simultaneously, antiviral and FcγR-mediated phagocytosis of immune-related genes was

induced under UV-B stress. These upregulated genes associated with immune responses indicate that many immune responses in insects can be activated under UV-B stress, illuminating the strong immune adaptive functions of insects [29, 35].

The sensing and transduction of intracellular stress signals are critical for the adaptation and survival of insects following exposure to UV-B radiation. Studies indicated that the PI3K-Akt pathway activates the nuclear factor erythroid 2 related factor 2 pathway, which is a key factor that protects cells against damage induced by UV-B by inhibiting oxidative stress [36]. Therefore, activation of the PI3K-Akt pathway may be critical in the insect response to UV-B stress. As an important pressure-sensing and energy-regulating factor, AMPK is essential for the survival of organisms in harsh environments. Under UV-B stress, the AMPK signaling pathway in M. persicae was activated, and this activation is related to its molecular adaptation mechanism under UV-B stress [37, 38]. Activation of the cGMP-PKG signaling pathway mobilizes intracellular Zn^{2+} to prevent mitochondrial oxidative damage in cardiomyocytes [39]. However, UV-B stress can cause significant ROS accumulation and damage to organisms. Activation of the cGMP-PKG signaling pathway can protect mitochondria in insect cells. These findings indicated that signal transduction plays an important role in the response of M. persicae to UV-B stress.

Conclusions

In summary, in this study, we used RNA-seq for the first time to narrate the genes associated with the adaptation of M. persicae to UV-B stress. The results illustrated that the adaptive mechanism of M. persicae to UV-B stress is complex, mainly involving genes involved in antioxidation, detoxification, metabolic and protein turnover, immune response, and stress signal transduction. Our results clarify the basis of the adaptive mechanism of insects in response to UV-B stress.

Methods

Insects rearing

M. persicae was raised by the Institute of Entomology, Guizhou University in chambers at a temperature of 25℃ ± 1℃ and relative humidity of 70%–80% under a 14-h/10-h photoperiod.

UV-B treatment

To exclude the influence of other light sources, *M. persicae* was fully dark adapted for 2 h, and specimens were then divided into two groups: UV-B radiation and control groups (3 replicates per group, 30 aphids per replicate). In the first group, specimens were irradiated with UV-B (280–320 nm) for 30 min at an intensity of 300 μW/cm^2. In the second group, specimens were irradiated using light-emitting diode fluorescent lamp bulbs for 30 min at the same intensity. The temperature and humidity during irradiation were consistent with the normal feeding conditions. Immediately after the end of treatment, insects were quickly frozen in liquid nitrogen and stored at −80℃ until RNA was extracted.

RNA isolation, library construction, and RNA sequencing (RNA-seq)

Total RNA in *M. persicae* was extracted using TRIzol® according the manufacturer's instructions (Invitrogen), and genomic DNA was removed using DNase I (TaKaRa). The RNA quality was determined using a 2100 Bioanalyzer (Agilent) and quantified using a ND-2000 (NanoDrop Technologies). The sequence library was constructed using only high-quality RNA samples (OD260/280 = 1.8–2.2, OD260/230 ≥ 2.0, RIN ≥ 6.5, 28S:18S ≥ 1.0, >10 μg).

The RNA-seq transcriptome library was constructed using a TruSeq™ RNA sample preparation kit (Illumina, San Diego, CA, USA). Poly-A mRNA was first enriched from 5 μg of total RNA using magnetic beads with oligo (dT). Then, fragmentation buffer was added to randomly degrade the mRNA into small fragments of approximately 200 bp. Next, double-stranded cDNA synthesis was performed with mRNA as a template using a SuperScript Double-Stranded cDNA Synthesis Kit (Invitrogen, CA) and a random hexamer primer (Illumina). The double-stranded cDNA structure was blunt-ended by adding End-Repair Mix (Enzymatics, USA), followed by addition of an "A" base at the 3' end to ligate the Y-shaped link. The specific procedure is described in the specification. After amplifying cDNA via 15 cycles of PCR, a 200–300-bp target band was recovered using 2% agarose gel. After quantification using TBS380 (Picogreen), the library was subjected to high-throughput sequencing using the Illumina HiSeq4000 sequencing platform with a sequencing read length of 2× 150 bp.

Sequence assembly

Quality control of raw data was achieved via sequencing using SeqPrep (https://github.com/jstjohn/SeqPrep) and Sickle (https://github.com/najoshi/sickle) with the default parameters (removing null reads, low quality fragments, and an unknown base pair N sequence) to obtain a pure sequence. Afterwards, clean reads were separately aligned to the *M. persicae* reference genome for assembly using TopHat software (http://tophat.cbcb.umd.edu/, version 2.0.0) [40].

Differential expression analysis and functional enrichment

To identify differentially expressed genes (DEGs) between two different samples, fragments per kilobase of transcript per million mapped reads (FPKM) were used to quantify gene expression, and the count of reads was further normalized to the FPKM values. The corresponding significance thresholds for fold change (FC) and *P-value* were estimated using standardized gene expression levels [determined by the control false discovery rate (FDR)]. Based on the expression level, the significance thresholds for DEGs in this study were FDR < 0.05 and FC > 1.5. In addition, the enrichment of DEGs was analyzed using GO and KEGG. GO functional enrichment and KEGG pathway analyses were performed using Goatools (https://github.com/tanghaibao/Goatools) and KOBAS 2.0 (http://kobas.cbi.pku.edu.cn/home.do) [41].

qRT-PCR verification

The 15 annotated unigenes were randomly selected for verification via qRT-PCR. Total RNA was extracted from specimens from each treatment group using TRIzol. The primers used for qRT-PCR are shown in

Table 3. cDNA was synthesized using a reverse transcription PrimeScript™ RT reagent kit (TaKaRa). qRT-PCR was performed on a C1000 real-time PCR system (Bio-Rad). In total, the 20 μL reaction mixture comprised 1 μL of cDNA (400 ng/μL), 10 μL of LYBR Green Supermix (TaKaRa), 1 μL of each of the primers (10 μmol/L), and 7 μL of ddH_2O. The $2^{-\Delta\Delta Ct}$ method was used to analyze the relative differences in transcription levels [42]. *Glyceraldehyde-3-phosphate dehydrogenase* (*GAPDH*) and *β-actin* were used as internal controls, and experiments were performed using three biological replicates.

Abbreviations

DEGs: Differentially expressed genes; CDS: Coding sequence; NR: NCBI non-redundant protein database; GO: Gene Ontology; KEGG: Kyoto Encyclopedia of Genes and Genomes; COG: Clusters of Orthologous Groups; Swiss-Prot: UniProtKB/Swiss-Prot; Pfam: Protein families database; FPKM: Fragments per kilobase of transcript per million; CYP: cytochrome P450; CTSB: Cathepsin B; ROS: Reactive oxygen species; TCA: tricarboxylic acid cycle; FC: Fold change; FDR: False Discovery Rate; qRT-PCR: Quantitative real-time PCR; RNA-seq: RNA sequencing; GAPDH: Glyceraldehyde-3-phosphate dehydrogenase.

Declarations

Ethics approval and consent to participate

Not applicable.

Consent for publication

Not applicable.

Availability of data and materials

RNA sequencing raw data have been deposited in the NCBI Sequence Read Archive (SRA; accession number PRJNA592018).

Competing interests

The authors declare that they have no competing interests.

Funding

This research was supported by the National Key R&D Program of China (2017YFD0200900) and the National Natural Science Foundation of China (31401754 and 31460483).

Authors' contributions

CLY and CYZ conceived this study. CLY and MSY collected data and data analyses. CLY and JYM contributed analysis tools. CLY and MSY carried out experiments. CLY and CYZ wrote the manuscript with help from all the authors. All authors read and approved the final manuscript.

Acknowledgements

We thank Majorbio (Shanghai, China) for technical assistance.

References

1. McKenzie RL, Aucamp PJ, Bais AF, Björn LO, Ilyas M. Changes in biologically-active ultraviolet radiation reaching the Earth's surface. Photochem Photobiol Sci. 2007;6:218-31.
2. Lidon FJC, Teixeira M, Ramalho JC. Decay of the chloroplast pool of ascorbate switches on the oxidative burst in UV-B-irradiated rice. J Agron Crop Sci. 2012;198:130-44.
3. Pitzschke A, Forzani C, Hirt H. Reactive oxygen species signaling in plants. Antioxid Redox Sign. 2006;8;1757-64.
4. Gill SS, Tuteja N. Reactive oxygen species and antioxidant machinery in abiotic stress tolerance in crop plants. Plant Physiol Bioch. 2010;48:909-30.
5. Jordan BR. Review: Molecular response of plant cells to UV-B stress. Funct Plant Biol. 2002;29:909-16.
6. Hideg É, Jansen MAK, Strid A. UV-B exposure, ROS, and stress: inseparable companions or loosely linked associates? Trends Plant Sci. 2013;18:107-15.
7. Sang W, Yu L, He L, Ma WH, Zhu ZH, Zhu F, Wang XP, Lei CL. UVB radiation delays *Tribolium castaneum* metamorphosis by influencing ecdysteroid metabolism. PLoS One. 2016;11:e0151831.
8. Villena OC, Momen B, Sullivan J, Leisnham PT. Effects of ultraviolet radiation on metabolic rate and fitness of *Aedes albopictus* and *Culex pipiens* mosquitoes. PeerJ. 2018;6:e6133.
9. Potter KA, Woods HA. Immobile and tough versus mobile and weak: effects of ultraviolet B radiation on eggs and larvae of *Manduca sexta*. Physiol Entomol. 2013;38:246-52.
10. Tuncbilek AS, Ercan FS, Canpolat U. Effect of ionizing (gamma) and non-ionizing (UV) radiation on the development of *Trichogramma euproctidis* (Hymenoptera: Trichogrammatidae). Arch Biol Sci. 2012;64:287-95.
11. Berlandier FA. Aphids on the world's crops. An information and identification guide. Austral Entomol. 2000;39:354-55.
12. Weber G. Genetic variability in host plant adaptation of the green peach aphid, *Myzus persicae*. Entomol Exp Appl. 1985;38:49-56.
13. Ogata H, Goto S, Sato K, Fujibuchi W, Bono H, Kanehisa M. KEGG: kyoto encyclopedia of genes and genomes. Nucleic Acids Res. 2000;27:29-34.

14. Del Río LA, Corpas FJ, Sandalio LM, Palma JM, Gómez M, Barroso JB. Reactive oxygen species, antioxidant systems and nitric oxide in peroxisomes. Exp. Bot. 2002;53:1255-72.
15. Liu Y, Su H, Li R, Li X, Xu Y, Dai X, Zhou Y, Wang H. Comparative transcriptome analysis of *Glyphodes pyloalis* Walker (Lepidoptera: Pyralidae) reveals novel insights into heat stress tolerance in insects. BMC Genomics. 2017;18:974.
16. Liu Y, Xin ZZ, Song J. Zhu XY, Liu QN, Zhang D Z, Tang BP, Zhou CL, Dai LS. Transcriptome analysis reveals potential antioxidant defense mechanisms in *Antheraea pernyi* in response to zinc stress. J Agric Food Chem. 2018;66:8132-41.
17. Howard AC, Mcneil AK, Mcneil PL. Promotion of plasma membrane repair by vitamin E. Nature Commun. 2011;2:597.
18. Meng JY, Zhang CY, Zhu F, Wang XP, Lei Ultraviolet light-induced oxidative stress: effects on antioxidant response of *Helicoverpa armigera* adults. J Insect Physiol. 2009;55:588-92.
19. Wang Y, Wang LJ, Zhu ZH, Ma WH, Lei CL. The molecular characterization of antioxidant enzyme genes in *Helicoverpa armigera* adults and their involvement in response to ultraviolet-a stress. J Insect Physiol. 2012;58:1250-8.
20. Coleman J, Blake-Kalff M, Davies E. Detoxification of xenobiotics by plants: chemical modification and vacuolar compartmentation. Trends Plant Sci. 1997;2:144-51.
21. Karunaratne SH, Hemingway J, Jayawardena KG, Dassanayaka V, Vaughan A. Kinetic and molecular differences in the amplified and non-amplified esterases from insecticide-resistant and susceptible *Culex quinquefasciatus* J Biol Chem. 1995;270:31124-8.
22. Feyereisen, R. Arthropod CYPomes illustrate the tempo and mode in P450 evolution. BBA-Proteins Proteom. 2011;1814:19-28.
23. Sang W, Ma WH, Qiu L, Zhu ZH, Lei CL. The involvement of heat shock protein and cytochrome P450 genes in response to UV-A exposure in the beetle *Tribolium castaneum*. J Insect Physiol. 2012;58:830-6.
24. Nguyen TTA, Michaud D, Cloutier C. A proteomic analysis of the aphid *Macrosiphum euphorbiae* under heat and radiation stress. Insect Biochem Molec. 2009;39:20-30.
25. Zhou LJ, Zhu ZH, Liu ZX, Ma WH, Desneux N, Lei CL. Identification and transcriptional profiling of differentially expressed genes associated with response to UVA radiation in *Drosophila melanogaster* (Diptera: Drosophilidae). Environ Entomol. 2013;42:1110-7.
26. Aguirre J, Hansberg W, Navarro R. Fungal responses to reactive oxygen species. Med Mycol. 2006;44:101-7.
27. Zhang X, St Leger RJ, Fang W. Stress-induced pyruvate accumulation contributes to cross protection in a fungus. Environ Microbiol. 2018;20:1158-69.
28. Theopold U, Dushay M. Mechanisms of *Drosophila* immunity-an innate immune system at work. Curr Immunol Rev. 2007;3:276-88.

29. Adamo SA. The effects of the stress response on immune function in invertebrates: an evolutionary perspective on an ancient connection. Horm Behav. 2012;62:324-30.
30. Cho WL, Tsao SM, Hays AR, Walter R, Chen JS, Snigirevskaya ES, Raikhel AS. Mosquito cathepsin B-like protease involved in embryonic degradation of vitellin is produced as a latent extraovarian precursor. J Biol Chem. 1999;274:13311-21.
31. Zhao XF, Wang JX, Xu XL, Schmid R, Wieczorek H. Molecular cloning and characterization of the cathepsin B-like proteinase from the cotton boll worm, *Helicoverpa armigera*. Insect Mol Biol. 2003;11:567-75.
32. Matsumoto I, Emori Y, Abe K, Arai S. Characterization of a gene family encoding cysteine proteinases of *Sitophilus zeamais* (Maize Weevil), and analysis of the protein distribution in various tissues including alimentary tract and germ cells. J Biochem. 1997;121:464-76.
33. Yamamoto Y, Zhao XF, Suzuki AC, Takahashi SY. Cysteine proteinase from the eggs of the silkmoth, *Bombyx mori*: site of synthesis and a suggested role in yolk protein degradation. J Insect Physiol. 1994;40:447-54.
34. Zhao XF, An XM, Wang JX, Dong DJ, Du XJ, Sueda S, Kondo H. Expression of the *Helicoverpa* cathepsin B-like proteinase during embryonic development. Arch Insect Biochem Physiol. 2005;58:39-46.
35. Adamo SA. Stress responses sculpt the insect immune system, optimizing defense in an ever-changing world. Dev Comp Immunol. 2017;66:24-32.
36. Zhang B, Zhao Z, Meng X, Chen H, Fu G, Xie K. Hydrogen ameliorates oxidative stress via PI3K-Akt signaling pathway in UVB-induced HaCaT cells. Int J Mol Med. 2018;41:3653-61.
37. Hardie DG. AMP-activated protein kinase—an energy sensor that regulates all aspects of cell function. Gene Dev. 2011;25:1895-908.
38. Zhu XJ, Feng CZ, Dai ZM, Zhang RC, Yang WJ. AMPK alpha subunit gene characterization in *Artemia* and expression during development and in response to stress. Stress. 2007;10:53-63.
39. Jang Y, Wang H, Xi J, Mueller RA, Norfleet EA, Xu Z. NO mobilizes intracellular Zn^{2+} via cGMP/PKG signaling pathway and prevents mitochondrial oxidant damage in cardiomyocytes. Cardiovasc Res. 2007;75:426-33.
40. Trapnell C, Pachter L, Salzberg SL. TopHat: discovering splice junctions with RNA-Seq. Bioinformatics. 2009;25:1105-11.
41. Xie C, Mao X, Huang J, Ding Y, Wu J, Dong S, Kong L, Gao G, Li CY, Wei L. KOBAS 2.0: a web server for annotation and identification of enriched pathways and diseases. Nucleic Acids Res. 2011;39:W316-22.
42. Livak KJ, Schmittgen TD. Analysis of relative gene expression data using real-time quantitative PCR and the $2^{-\Delta\Delta CT}$ Methods. 2001;25:402-08.

Tables

Table 1 Statistical analysis of transcriptome sequencing data

Sample		CK	U30
Clean reads	Total clean reads	80,281,002	90,660,496
	Total clean base pairs	11,790,769,793	13,279,045,152
	Q30 of clean reads	93.17%	92.53%
	GC count	41.6%	41.5%
Mapping to genome	Total mapped reads	77,563,631 (96.62%)	87,925,513 (96.98%)
	Multiple mapped reads	2,521,212 (3.14%)	2,506,308 (2.76%)
	Uniquely mapped reads	75,042,419 (93.47%)	85,419,205 (94.22%)
Distribution of reads in different regions	Introns	1,949,073 (1.620%)	2,702,377 (2.01%)
	3'UTR	5,647,225 (4.70%)	5,904,505 (4.40%)
	5'UTR	7,317,961 (6.10%)	9,438,718 (7.03%)
	CDS	100,508,905 (83.72%)	112,142,662 (83.48%)

Table 2 RNA sequencing results for gene expression in the two groups

Category	CK	U30
Highly expressed genes	7,058	6,611
Medium expressed genes	3,455	3,764
Low expressed genes	3,724	4,073
Total expressed genes	14,237	14,448
Unexpressed genes	3,258	2,772

Table 3 List of qRT-PCR primers

Gene_name	Forward primer (5′–3′)	Reverse primer (5′–3′)	Gene description
LOC111037390	AGCAATCAGTTTAAGCCCCT	AGGTGCGTTAAGCAACCTGA	UDP-glucuronosyltransferase 2B17-like
LOC111030222	AGAGTCACGAGTATCAGCCC	GGTGCACTCAAAGCGTACAA	short-chain dehydrogenase/reductase-like
LOC111037735	TCCGCGATCCTGAAATCATC	TTTCCCGATGTGAATGCTGG	cytochrome P450 protein
LOC111036713	TGCTTCCAGTTGGGCTGTAG	TCGCCGCAAGACATAAGGTT	TPA_inf: cathepsin B
LOC111033945	ATGCCAGATGGTGAAGTGGA	AACGCGAATTATCCAACCGT	methyltransferase-like protein 13
LOC111041660	GACCCTCATAGTTGGTCAGC	CCCACGTAAGTGGTAGGGTA	gamma-glutamyl hydrolase A-like
LOC111028794	CGATAGGTACAGCATCCGCT	CGTCCGGATATTCGCCCATAA	cationic amino acid transporter 3-like
LOC111034979	TAGGATATGCCGCTCAAGGC	GAATTCGGCAGATGCAGACG	phosphate carrier protein, mitochondrial-like
LOC111036844	TGCTCGTGTCACTGGAGTTC	AGCTGTTCCGTCTCTGTTGG	muscle M-line assembly protein unc-89 isoform X5
LOC111028217	TCGTGCAACAAGAGCACTCA	TGCTTGCTACTCTGTCACTGG	very long-chain specific acyl-CoA dehydrogenase, mitochondrial
LOC111030399	CAACCATCATCCAGGACGGA	GTCATCGACAGTCAGGACCA	MPA13 allergen-like isoform X1
LOC111035011	CTGGACGACTGTAGGAAGCC	TTCGTCGGTGTCCTTGTACG	alpha-tocopherol transfer protein
LOC111036013	CCATGGCACTTCTAGAGTCAGG	ATCGAGCTCAGTGCTTCTGTC	acylphosphatase, putative

LOC111040667	TATCGCCACCGATAACGAGC	CCAAGCACAAGCCAACACAG	putative fatty acyl-CoA reductase CG5065
LOC111040115	GACGAGTACAAGAGGAGGCG	CCTGAGCACGTTGAGTTCCT	CCAAT/enhancer-binding protein
β-actin	TGGTATCGTCTTGGATTCTG	TTAGGTAGTCGGTGAGATCA	
GAPDH	TCACGCAATGACCTCCTCTC	CAGTGACACGTCCAGCGTAG	

Figures

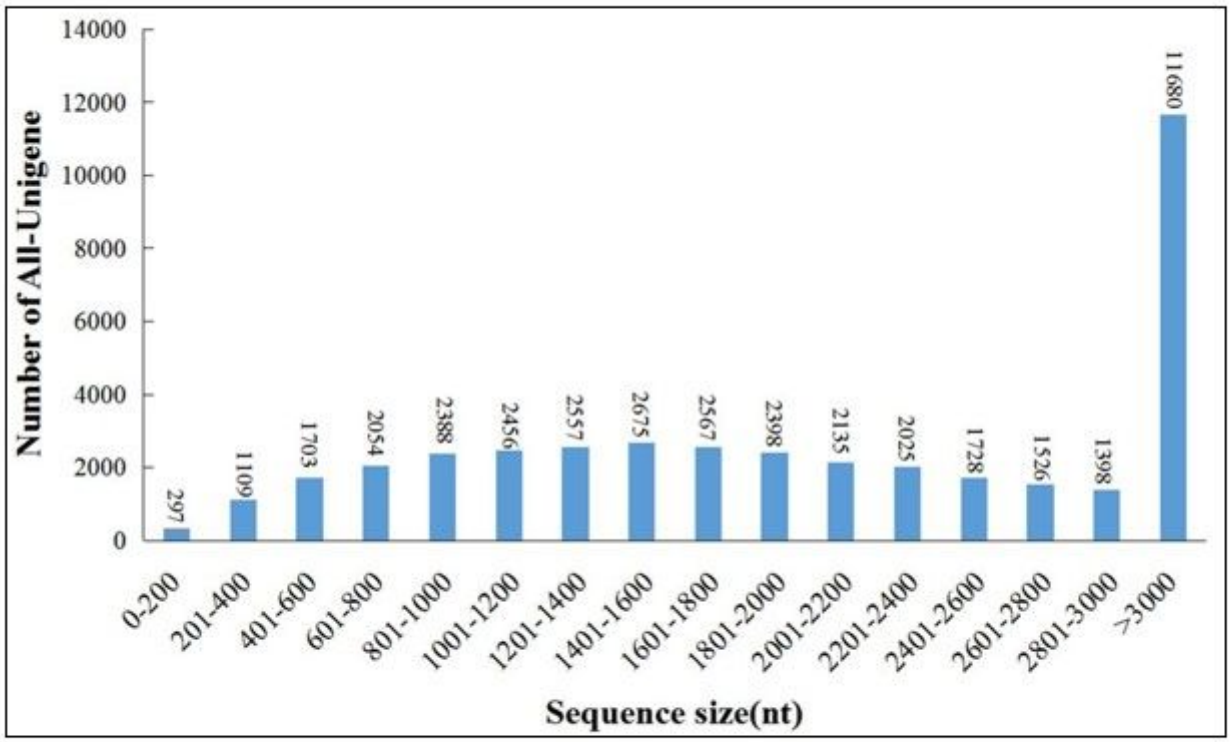

Fig. 1

Figure 2

Length distribution of the unigenes in the Myzus persicae transcriptome.

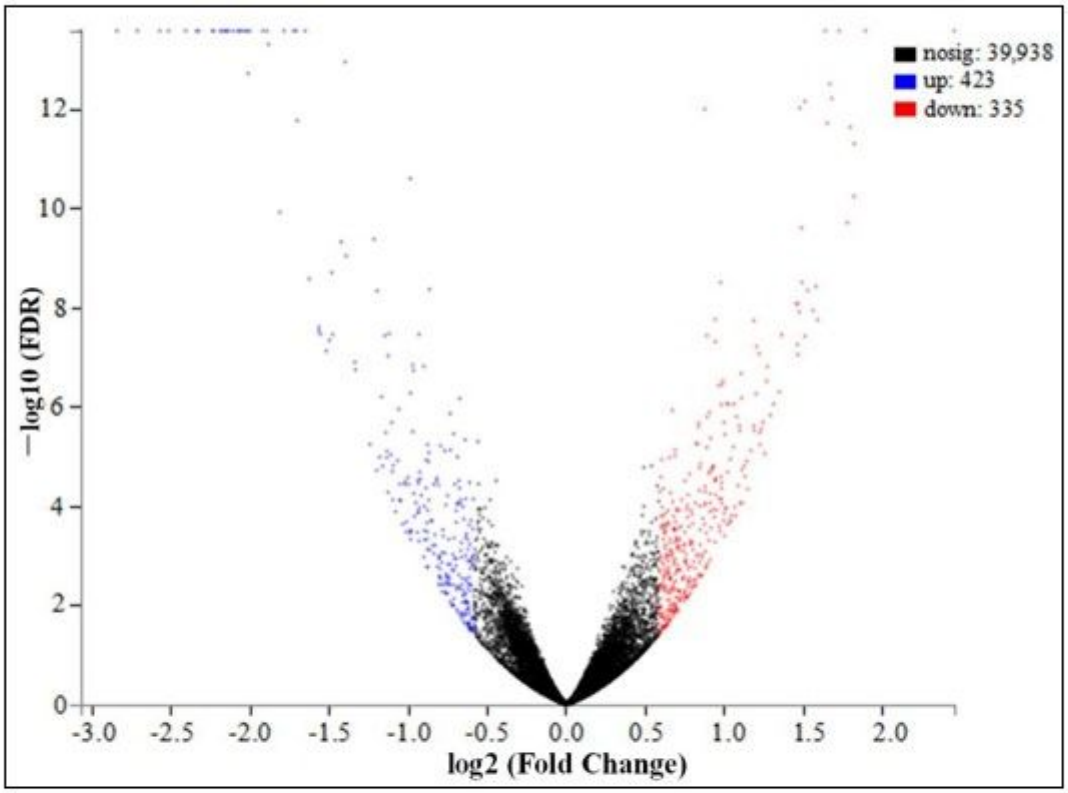

Fig. 2

Figure 4

Volcano plot of differentially expressed genes. The Y-axis presents −log10 significance. The X-axis presents log2 (fold change). Dots represent individual genes. Red dots represent upregulated genes, and blue dots denote downregulated genes. Black dots indicate genes that were not differentially expressed.

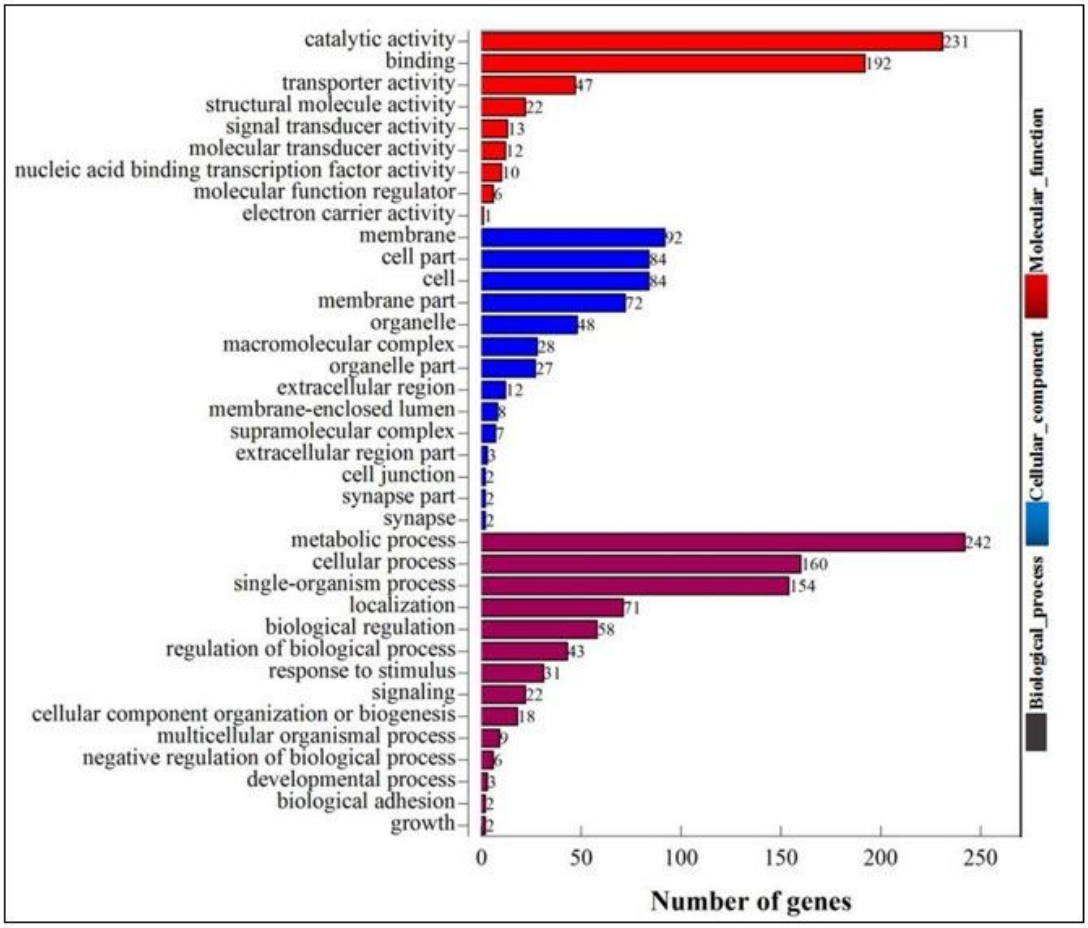

Fig. 3

Figure 6

Gene ontology enrichment of differentially expressed genes (DEGs) in Myzus persicae transcriptome under ultraviolet-B stress. All DEGs were grouped into three categories: biological process, cellular component, and molecular function.

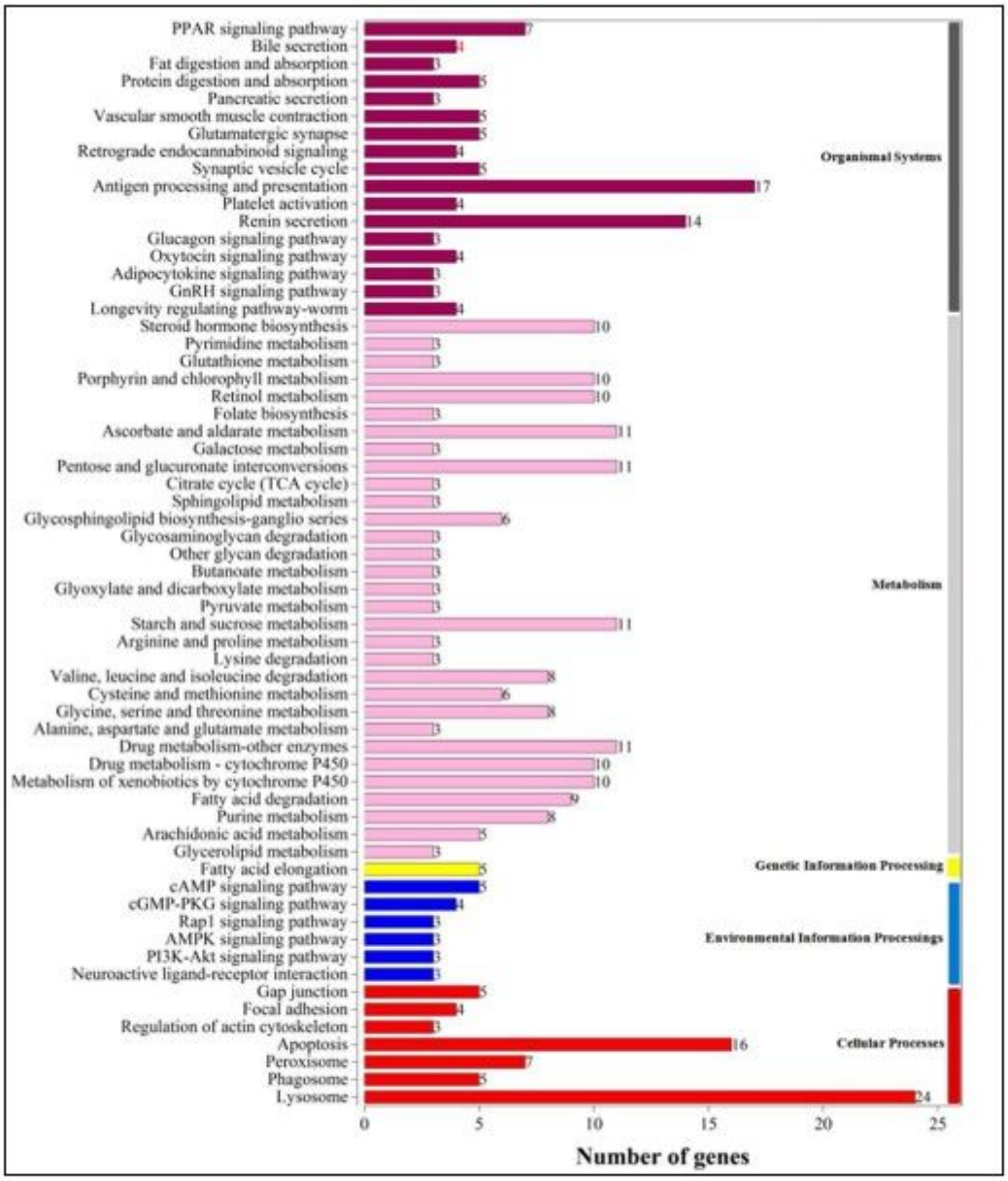

Fig. 4

Figure 7

Kyoto Encyclopedia of Genes and Genomes (KEGG) classification analysis of differentially expressed genes. Top 62 pathways according to enrichment factor as shown. The vertical axis presents the enriched KEGG pathways, and the horizontal axis presents the number of unigenes in each pathway.

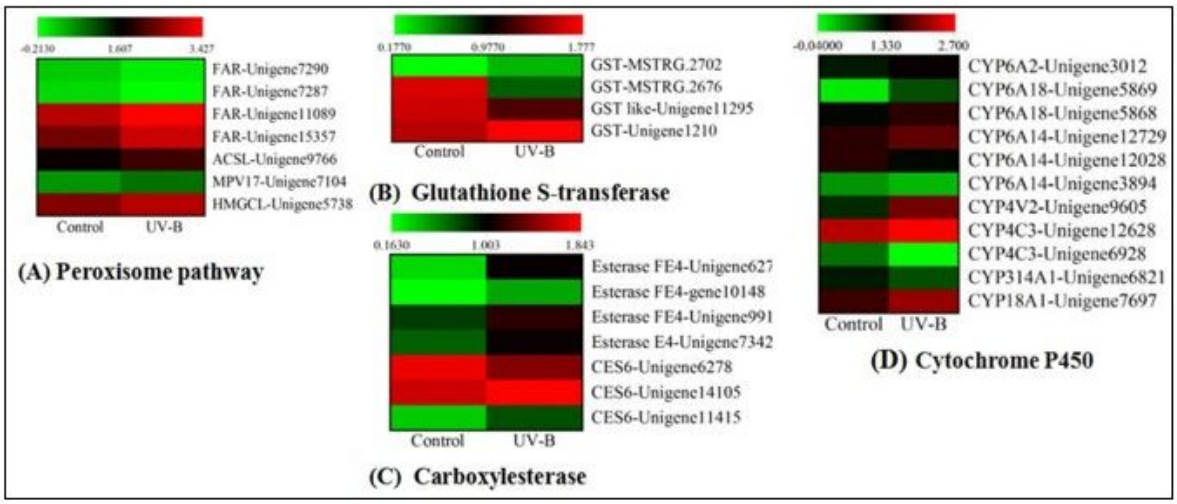

Fig. 5

Figure 9

Heatmap of antioxidation and detoxification gene expression under ultraviolet-B radiation. The expression levels of peroxisome pathway, glutathione S-transferase, carboxylesterase, and cytochrome P450 genes are presented in A, B, C, and D, respectively. The color scale is shown at the upper left, spanning from the lowest (green) to the highest (red) log10 (expression) value.

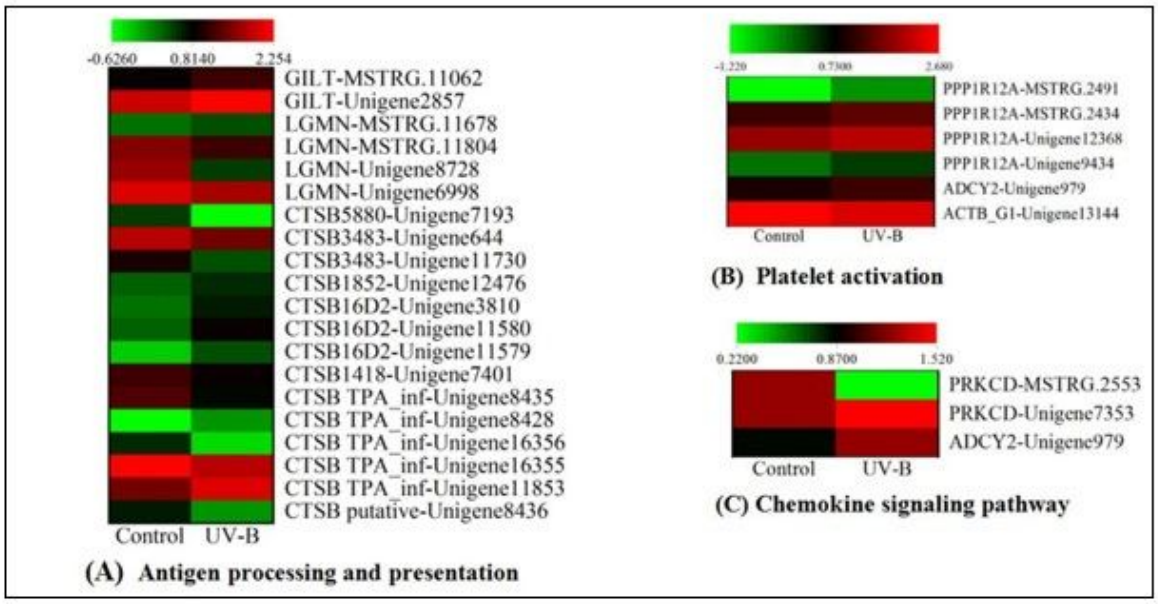

Fig. 6

Figure 12

Heatmap of immune response gene expression under ultraviolet-B radiation. The antigen processing and presentation, platelet activation, and chemokine signaling pathways are shown in A, B, and C, respectively. The color scale is shown at the upper left, spanning from the lowest (green) to the highest (red) log10 (expression) value.

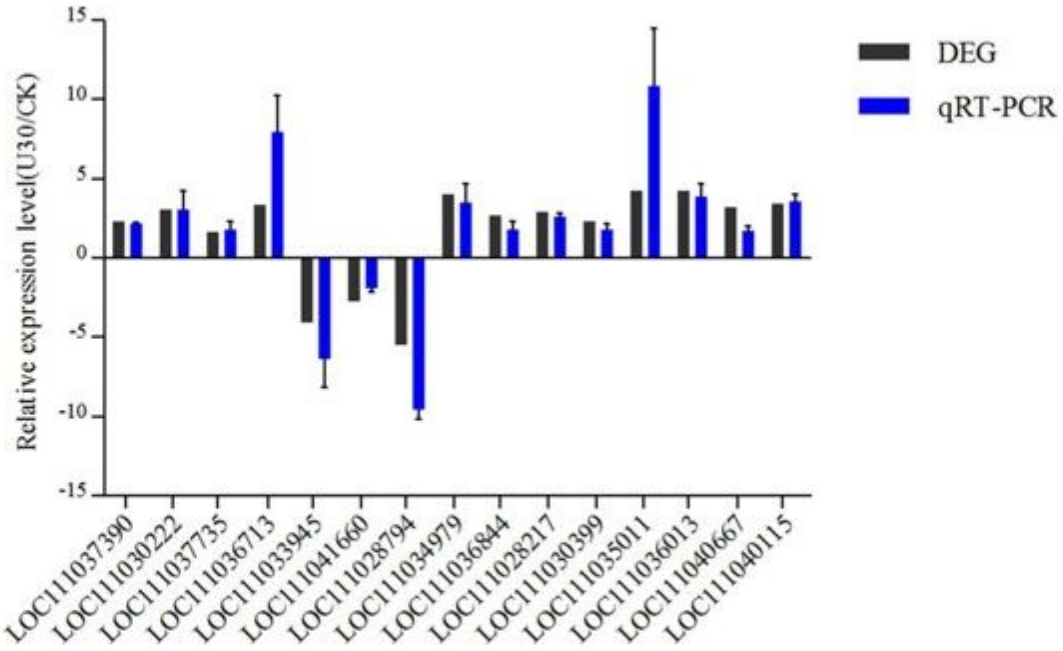

Fig. 7

Figure 14

qRT-PCR validation of differentially expressed genes (DEGs) in M. persicae under ultraviolet-B stress. DEGs were identified via RNA sequencing. The X-axis presents different unigenes. The Y-axis presents the relative expression levels of genes. Glyceraldehyde-3-phosphate dehydrogenase and β-actin were used as internal controls.